Available online at www.sciencedirect.com
SCIENCE DIRECT®
Journal of Power Sources 129 (2004) 205–215
JOURNAL OF POWER SOURCES
www.elsevier.com/locate/jpowsour

Modeling SOFC plants on the distribution system using identification algorithms

Francisco Jurado*
[a] *Department of Electrical Engineering, University of Jaén, 23700 EPS Linares (Jaén), Spain*

Received 16 July 2003; received in revised form 6 November 2003; accepted 15 November 2003

Abstract

To determine the potential impacts of fuel cells on future distribution system, dynamic models of fuel cells should be created, reduced in order, and scattered throughout test feeders.

This paper presents the implementation of an efficient method for computing low-order linear system models of solid oxide fuel cells (SOFCs) from time domain simulations. The method is the Box–Jenkins algorithm for calculating the transfer function of a linear system from samples of its input and output.

Keywords: Solid oxide fuel cells; Box–Jenkins algorithm; Linear system

1. Introduction

Exhibiting the dynamic influences of solid oxide fuel cell (SOFC) on the distribution grid requires the use of a large dynamic model [1]. Since SOFCs will be proliferated, it is necessary to reduce the model order of each SOFC system to enable computational analysis.

The computation of linear system models of power systems from time domain simulations is a topic of considerable practical interest. This interest is motivated by the insight into the dynamic interactions among power system components that can be obtained from a linear representation. Linear models allow for the application of linear analysis techniques to complement the information obtained from nonlinear time domain simulations and often allow for a better understanding of the system dynamic characteristics than that obtained from the inspection of time simulations alone. Although the nonlinear nature of a SOFC must be recognized, in many cases a linearized system representation allows for a more efficient means of analysis.

Several techniques for computing state space matrices and transfer function realizations of power systems from time domain data have been proposed in recent years. These techniques include the Prony method which is based on fitting a weighted sum of exponential terms to a given signal [2], methods based on FFT analyses [3], and the eigensystem realization algorithm [4]. In addition, methods designed to estimate the frequency response of a system have also been proposed [5]. The Prony method is perhaps the method for which more extensive results and applications have been documented. Its application to the analysis and control of electromechanical oscillations has shown the value of deriving linear models from time domain simulations and measured data [6].

This paper presents the application of the Autoregression with exogenous signal (ARX) identification algorithm to compute low-order system models, suitable for analysis and control design [7–9]. This algorithm consists of a simple procedure for calculating the transfer function of a linear system from samples of its input and output.

Using MATLAB/Simulink [10], a dynamic model of a SOFC-penetrated distribution system is created.

This paper is structured as follows. Section 2 presents a review of the SOFC. Section 3 introduces the utility-connected inverter control. Some basic concepts of ARX models are described in Section 4. Section 5 compares the response of identified system versus the response of the actual system. Section 6 depicts some simulation results. Finally, conclusions are presented in Section 7.

2. Solid oxide fuel cell

Most likely, fuel cell will be a dominant distributed energy resource. The SOFCs are dynamic devices and when

* Corresponding author. Tel.: +34-953-026518; fax: +34-953-026508.
E-mail address: fjurado@ujaen.es (F. Jurado).

0378-7753/$ – see front matter © 2003 Elsevier B.V. All rights reserved.
doi:10.1016/j.jpowsour.2003.11.035

Nomenclature

Fuel cell

E_0	ideal standard potential
F	Faraday's constant
I_{fc}	fuel cell current
K_{an}	anode valve constant
K_{H_2}	valve molar constant for hydrogen
K_{H_2O}	valve molar constant for water
K_{O_2}	valve molar constant for oxygen
K_r	constant ($=N_0/4F$)
M_{H_2O}	molecular mass of hydrogen
n_{H_2}	number of hydrogen moles in the anode channel
N_0	number of cells in series in the stack
p_i	partial pressure
P	real power
P^*	set point for the real power
$q^{in}_{H_2}$	input fuel flow
$q^{o}_{H_2}$	output fuel flow
$q^{r}_{H_2}$	fuel flow that reacts
r	ohmic loss
r_{H-O}	ratio of hydrogen to oxygen
R	universal gas constant
T	absolute temperature
T_e	electrical response time
T_f	fuel processor response time
U	fuel utilization
V_{an}	volume of the anode
V_{fc}	fuel cell voltage
τ_{H_2}	response time for hydrogen flow
τ_{H_2O}	response time for water flow
τ_{O_2}	response time for oxygen flow

Inverter

E	load bus voltage
E^*	set point for the load bus voltage
L_T	inductance
Q	reactive power
Q^*	set point for the reactive power
V	inverter output voltage space vector
X_T	reactance ($=L_T\omega$)
δ_p	angle between ψ_v and ψ_e
δ^*_p	angle reference
ψ_e	flux vector associated with E
ψ_v	flux vector associated with V
ψ^*_v	flux vector reference

connected to the distribution system they will affect its dynamic behavior. Hence, researchers have developed dynamic models for these components [11–15].

The chemical response in the fuel processor is usually slow. It is associated with the time to change the chemical reaction parameters after a change in the flow of reactants. This dynamic response function is modeled as a first-order transfer function with a 5 s time constant.

The electrical response time in the fuel cells is generally fast and mainly associated with the speed at which the chemical reaction is capable of restoring the charge that has been drained by the load. This dynamic response function is also modeled as a first-order transfer function but with a 0.8 s time constant.

With aid of the inverter, the fuel cell system can supply not only real power but also reactive power. Usually, power factor can be in the range of 0.8–1.0. The SOFC system dynamic model is given in Fig. 1.

The fuel utilization (U) is the ratio between the fuel flow that reacts and the input fuel flow as follows:

$$U = \frac{q^{in}_{H_2} - q^{o}_{H_2}}{q^{in}_{H_2}} = \frac{q^{r}_{H_2}}{q^{in}_{H_2}} \tag{1}$$

Typically, an 80–90% fuel utilization is used.

Every individual gas will be considered separately, and the perfect gas equation will be applied to it. Hydrogen will be considered as an example

$$p_{H_2} V_{an} = n_{H_2} RT \tag{2}$$

It is possible to isolate the pressure and to take the time derivative of the previous expression, obtaining

$$\frac{dp_{H_2}}{dt} = \frac{RT}{V_{an}} q_{H_2} \tag{3}$$

There are three relevant contributions to the hydrogen molar flow: the input flow, the flow that takes part in the reaction and the output flow, thus

$$\frac{dp_{H_2}}{dt} = \frac{RT}{V_{an}} (q^{in}_{H_2} - q^{o}_{H_2} - q^{r}_{H_2}) \tag{4}$$

According to the basic electrochemical relationships, the molar flow of hydrogen that reacts can be calculated as

$$q^{r}_{H_2} = \frac{N_0 I}{2F} = 2K_r I^{r}_{fc} \tag{5}$$

Returning to the calculation of the hydrogen partial pressure, it is possible to write

$$\frac{dp_{H_2}}{dt} = \frac{RT}{V_{an}} (q^{in}_{H_2} - q^{o}_{H_2} - 2K_r I^{r}_{fc}) \tag{6}$$

If it could be considered that the molar flow of any gas through the valve is proportional to its partial pressure inside the channel, according to the expressions:

$$\frac{q_{H_2}}{p_{H_2}} = \frac{K_{an}}{\sqrt{M_{H_2}}} = K_{H_2} \tag{7}$$

Replacing the output flow by (7), taking the Laplace transform of both sides and isolating the hydrogen partial pressure, yields the following expression:

$$p_{H_2} = \frac{1/K_{H_2}}{1 + \tau_{H_2} s} (q^{in}_{H_2} - 2K_r I^{r}_{fc}) \tag{8}$$

where $\tau_{H_2} = V_{an}/K_{H_2} RT$.

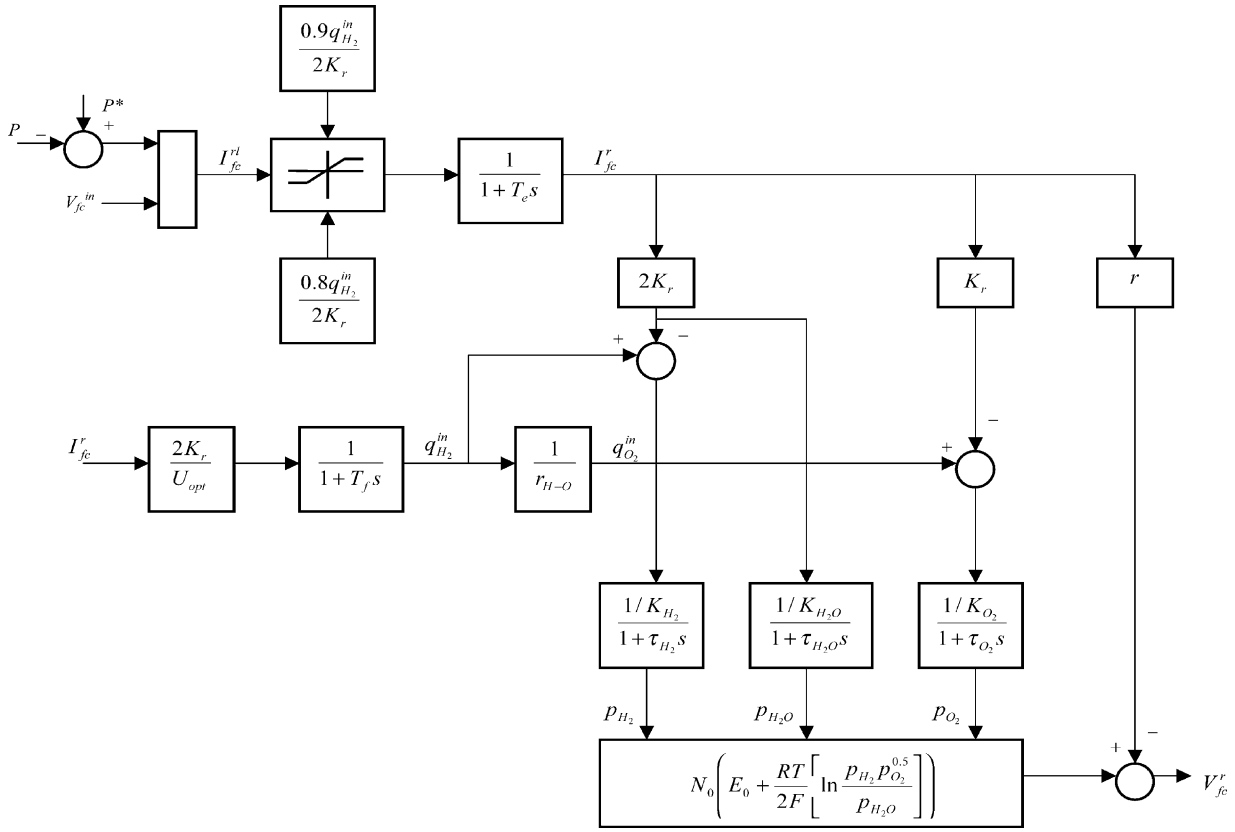

Fig. 1. SOFC system dynamic model.

A similar operation can be made for all the reactants and products. Applying Nernst's equation and Ohm's law (to consider ohmic losses), the stack output voltage is represented by the following expression:

$$V = N_0\left(E_0 + \frac{RT}{2F}\left[\ln\frac{p_{\mathrm{H_2}}p_{\mathrm{O_2}}^{0.5}}{p_{\mathrm{H_2O}}}\right]\right) - rI^{\mathrm{r}}_{\mathrm{fc}} \tag{9}$$

3. Utility-connected inverter control

Control of the flux vector has been shown to have good dynamic and steady-state performance [16]. It also provides a convenient means to define the power angle since the inverter voltage vector switches position in the *d–q* plane, whereas there is no discontinuity in the inverter flux vector.

For a six-pulse voltage source inverter (VSI), the inverter output voltage space vector can take any of the seven positions in the plane specified by the *d–q* coordinates. The time integral of the inverter output voltage space vector is called the "inverter flux vector" for short. The *d*- and *q*-axes components of the inverter flux vector ψ_v are defined as

$$\psi_{dv} = \int_{-\infty}^{t} v_d\,\mathrm{d}\tau, \qquad \psi_{dq} = \int_{-\infty}^{t} v_q\,\mathrm{d}\tau \tag{10}$$

The magnitude and the angle of ψ_v with respect to the *q*-axis are determined as

$$|\psi_v| = \sqrt{\psi_{qv}^2 + \psi_{dv}^2}, \qquad \delta_v = \tan^{-1}\left(\frac{-\psi_{dv}}{\psi_{qv}}\right) \tag{11}$$

The *d*- and *q*-axes components of the ac system voltage flux vector ψ_e, its magnitude, and angle are defined in a similar manner. The angle between ψ_v and ψ_e is defined as

$$\delta_p = \delta_v - \delta_e \tag{12}$$

It is useful to develop the power transfer relationships in terms of the flux vectors. The basic real power transfer relationship for the control system of Fig. 2 in the *d–q* reference frame is

$$P = \tfrac{3}{2}(e_q i_q + e_d i_d) \tag{13}$$

In (13), e_q and e_d are the *q*- and *d*-axes components, respectively, of the ac system voltage vector *E*. In addition, i_q and i_d are the components of the current vector *I*. When i_q and i_d are expressed in terms of the fluxes, taking into account the spatial relationships between the two flux vectors and assuming the ac system voltage to be sinusoidal, (13) can be expressed as

$$P = \frac{3}{2L_T}\omega\psi_e\psi_v\sin\delta_p \tag{14}$$

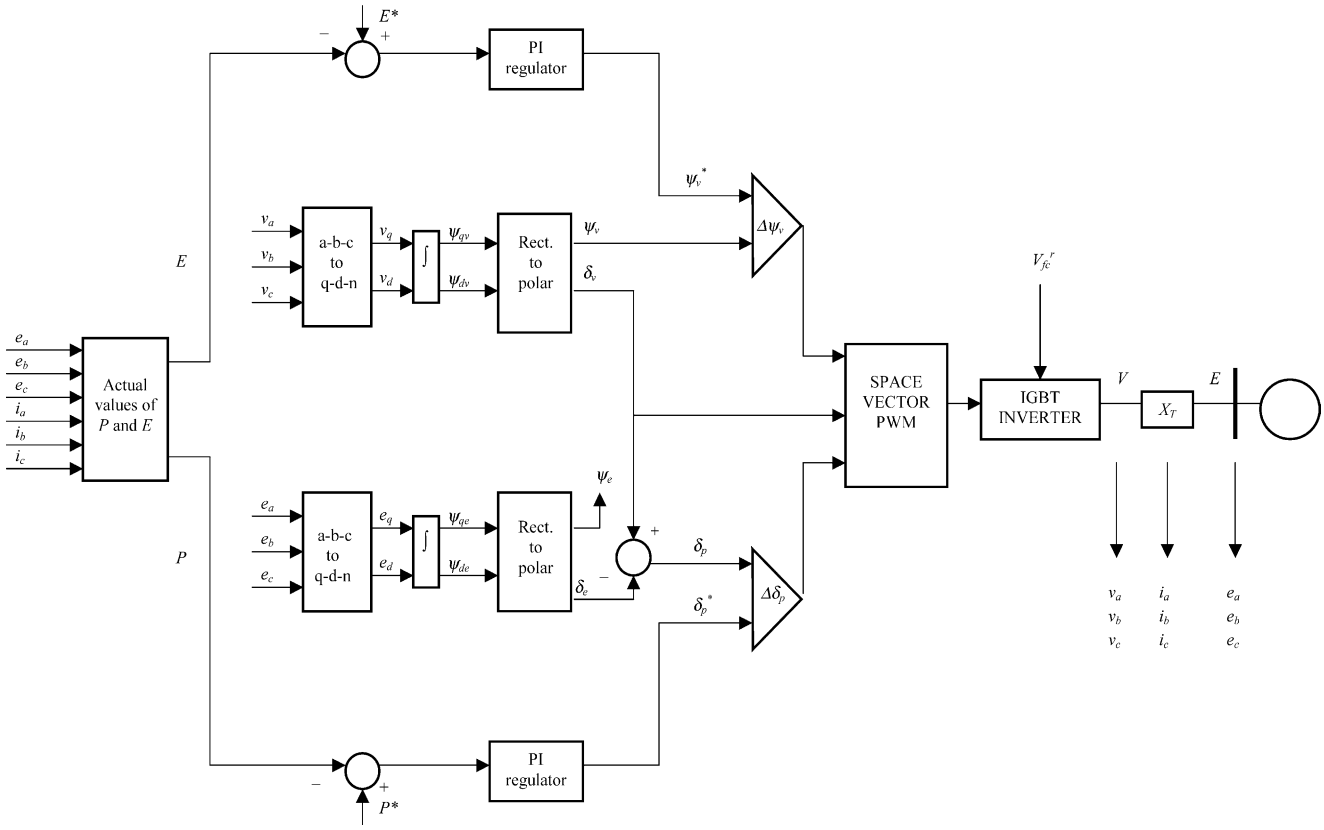

Fig. 2. Control system for the inverter.

In this expression ψ_e and ψ_v are the magnitudes of the ac system and the inverter flux vectors, respectively, and δ_p is the spatial angle between the two flux vectors. i is the frequency of rotation of the two flux vectors. The expression for reactive power transfer can be derived in a similar manner. This is

$$Q = \frac{3\omega}{2L_T}[\psi_e\psi_v \cos\delta_p - \psi_e^2] \tag{15}$$

Eqs. (14) and (15) indicate that P can be controlled by controlling δ_p, which can be defined as the power angle, and Q can be controlled by controlling ψ_v.

The two variables that are controlled directly by the inverter are ψ_v and δ_p. The vector ψ_v is controlled to have a specified magnitude and a specified position relative to the ac system flux vector ψ_e.

The errors between actual and desired amounts activate the remainder of the firing scheme only if they exceed a threshold value. If the error is larger than the hysteresis band (whose widths are $\Delta\delta_p$ and $\Delta\psi_v$) then a decision towards a new switching sequence is made. If the errors are within their hysteresis band, the switches will hold their current status.

Therefore, the SOFC plant has two major control loops:

1. *Power control*: done by adjusting the set point P^* of the inverter for fast transient variations and fuel flow input control for slow variations.
2. *Voltage control*: done by adjusting the set point E^* of the inverter, which effects the magnitude of the converter output voltage.

4. Identification algorithms

4.1. ARX models

The most used model structure is the simple linear difference equation

$$y(t) + a_1 y(t-1) + \cdots + a_{na} y(t-na) = b_1 u(t-nk) + \cdots + b_{nb} u(t-nk-nb+1) + e(t) \tag{16}$$

which relates the current output $y(t)$ to a finite number of past outputs $y(t-k)$ and inputs $u(t-k)$.

The structure is thus entirely defined by the three integers *na*, *nb*, and *nk*. *na* is equal to the number of poles and $nb-1$ is the number of zeros, while *nk* is the pure time-delay (the dead-time) in the system. For a system under sampled-data control, typically *nk* is equal to 1 if there is no dead-time.

For multi-input systems *nb* and *nk* are row vectors, where the *i*th element gives the order/delay associated with the *i*th input.

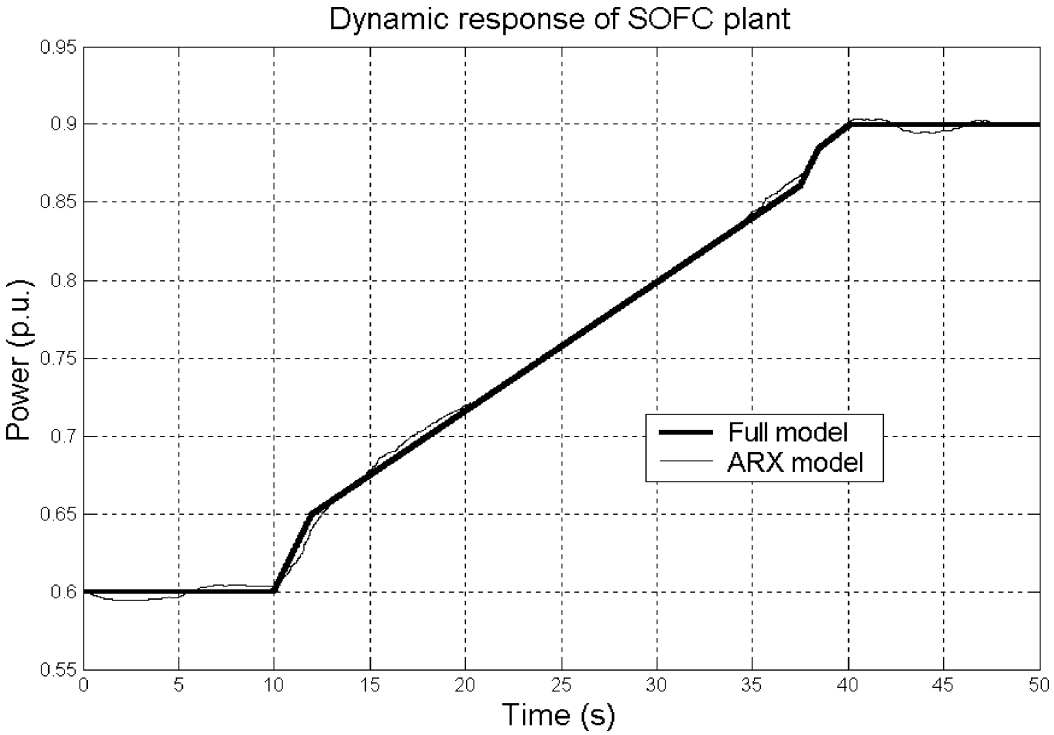

Fig. 3. Model output comparison.

There are two methods to estimate the coefficients *a* and *b* in the ARX model structure:

- *Least squares*: Minimizes the sum of squares of the right-hand side minus the left-hand side of the expression above, with respect to *a* and *b*.
- *Instrumental variables*: Determines *a* and *b* so that the error between the right- and left-hand sides becomes uncorrelated with certain linear combinations of the inputs.

4.2. ARMAX, output-error and Box–Jenkins models

There are several elaborations of the basic ARX model, where different disturbance models are introduced. These

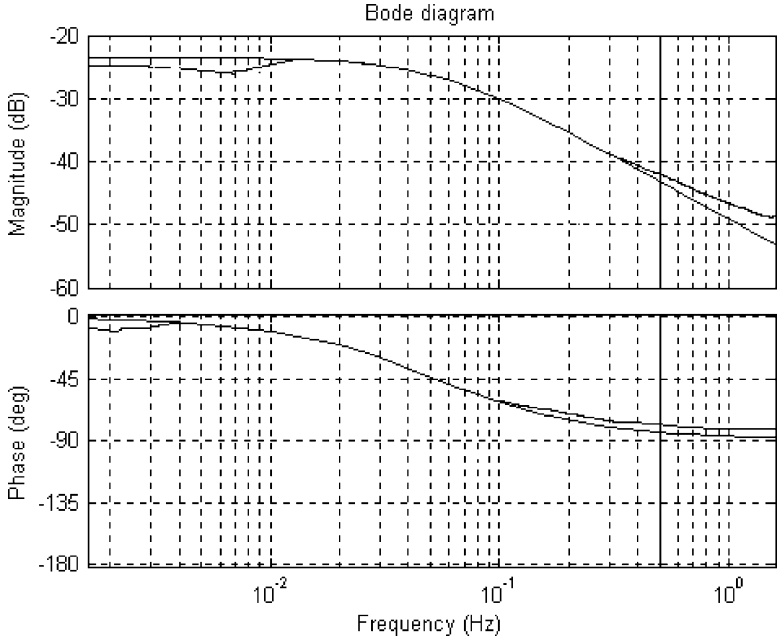

Fig. 4. Transfer function magnitude and phase comparison. Actual system and identified system.

include well known model types, such as ARMAX, output-error, and Box–Jenkins [17–19].

A general input–output linear model for a single-output system with input u and output y can be written as

$$A(q)y(t) = \sum_{i=1}^{nu}[B_i(q)F_i(q)]u_i(t - nk_i) + \left[\frac{C(q)}{D(q)}\right]e(t) \tag{17}$$

Here u_i denotes input #i, and A, B_i, C, D, and F_i are polynomials in the shift operator (z or q). It is just a compact way of writing difference equations.

The general structure is defined by giving the time-delays nk and the orders of these polynomials (i.e., the number of poles and zeros of the dynamic model from u to y, as well as of the disturbance model from e to y).

Most often the choices are confined to one of the following special cases:

$$\text{ARX}: \quad A(q)y(t) = B(q)u(t - nk) + e(t) \tag{18}$$

$$\text{ARMAX}: \quad A(q)y(t) = B(q)u(t - nk) + C(q)e(t) \tag{19}$$

$$\text{Output-error}: \quad y(t) = \left[\frac{B(q)}{F(q)}\right]u(t - nk) + e(t) \tag{20}$$

$$\text{Box–Jenkins}: \quad y(t) = \left[\frac{B(q)}{F(q)}\right]u(t - nk) + \left[\frac{C(q)}{D(q)}\right]e(t) \tag{21}$$

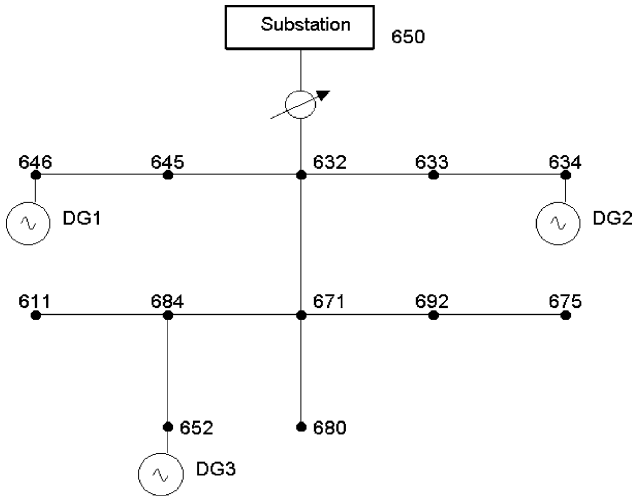

Fig. 5. One line diagram of IEEE 13 node feeder with fuel cells.

Note that $A(q)$ corresponds to poles that are common between the dynamic model and the disturbance model. Likewise $F_i(q)$ determines the poles that are unique for the dynamics from input #i, and $D(q)$ the poles that are unique for the disturbances.

Although each method has a somewhat different set of parameters that a system analyst can adjust, one requirement an identified system must meet is that its response to a given input should match the response of the actual system. This practical criterion was used as a guideline to adjust the order of the identified systems.

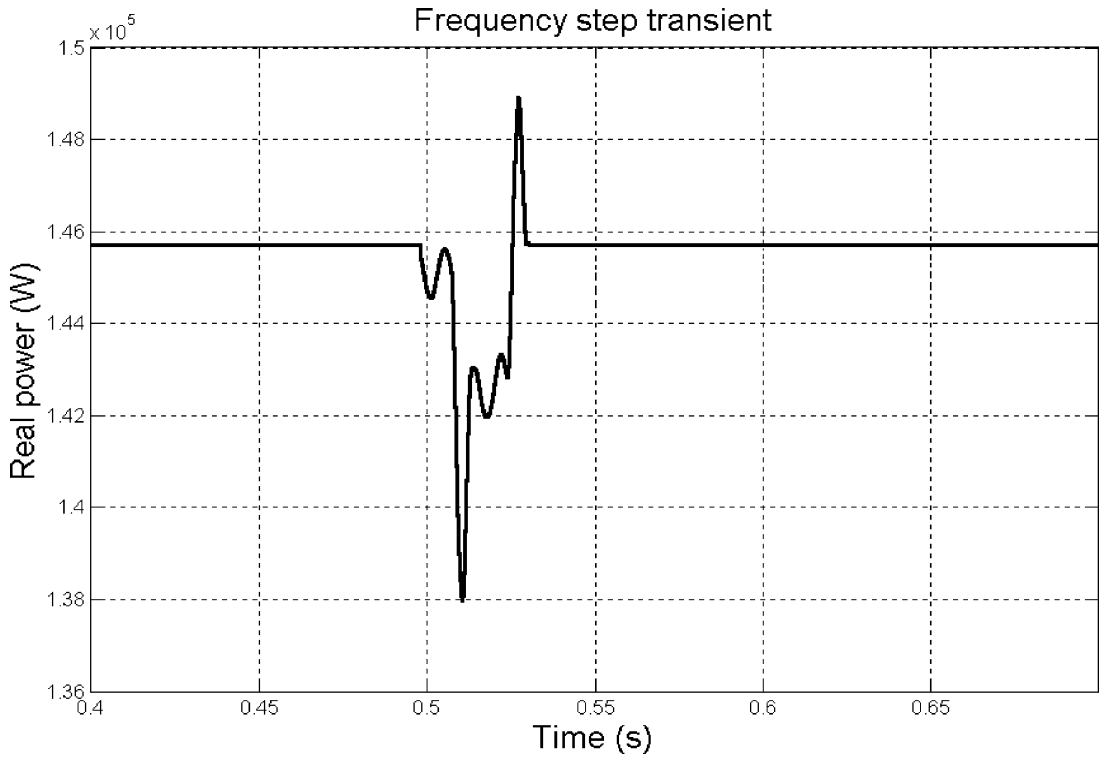

Fig. 6. Fuel cell response to a frequency step transient at node 634 for the IEEE 13 node feeder. Real power.

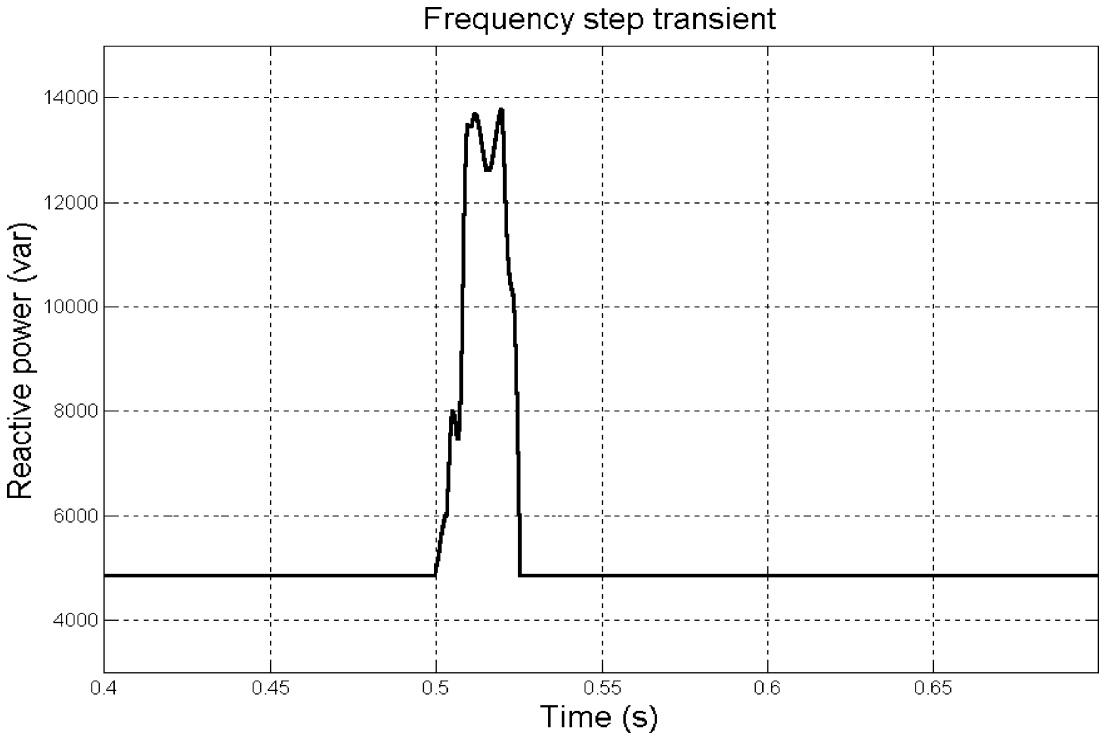

Fig. 7. Fuel cell response to a frequency step transient at node 634 for the IEEE 13 node feeder. Reactive power.

5. Performance

SOFC models used in the distribution system analysis were constructed as shown in the following:

- There is one 4.16 kV/480 V transformer.
- All SOFCs were connected at the end of their respective feeders at 480 V.

In this paper SOFC modeled is denoted as "the actual system". Once an identified system was obtained, its time domain response and transfer function were compared against the corresponding quantities of the actual system. To accomplish this, the actual system was linearized around an operating point.

The results presented here correspond to a 0.02 p.u. by 0.1 s probing pulse into the real power block of SOFC in

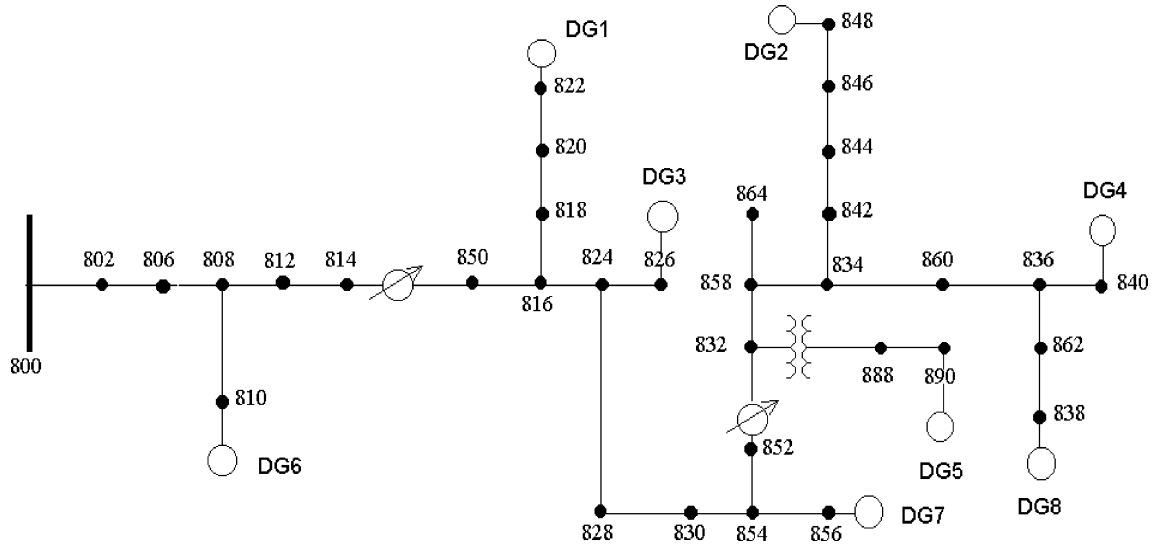

Fig. 8. One line diagram of IEEE 34 node feeder with fuel cells.

Fig. 1. The sampling time was 0.01 s and 600 points were used to perform the system identification.

Assume a SOFC is operating with constant rated voltage and power demand 0.6 p.u. There is 0.3 p.u. of step increase in the total load at $t = 10$ s.

Fig. 3 compares the time response of identified system versus the response of the actual system. The identified system was obtained using Box–Jenkins algorithm, and is of fourth order. This method estimates parameters of the Box–Jenkins model structure using a prediction error method. The order of the identified system is the minimum order required to obtain a good time domain match.

Fig. 4 compares the magnitude and phase of the transfer function $V_{fc}^{r}(s)/P(s)$ of the identified and the linearized actual systems. These plots show a very good match in the frequency range.

6. Simulation results

The IEEE test feeders [20] are used as the test system to investigate the dynamic characteristics of the distribution system with fuel cells. Figs. 5, 8 and 10 show the test systems with the fuel cells.

In this paper, all loads are balanced, and characterized by constant power.

The majority of data for the fuel cell model has been extracted from Kuipers and Singhal [21,22], and a commercial leaflet describing a SOFC 100 kW plant.

Here, all fuel cells in the test feeders have the same dynamic response and share the generation equally. The IEEE 13 node test feeder is very small, short and relatively highly loaded for a 4.16 kV feeder. Penetration means the proportion of the distribution feeder load being supplied by SOFCs associated with the distribution feeder [23]. In this model, an initial load of P_i is assumed and the penetration is thus,

$$\text{Penetration} = \frac{P}{P + P_i} \tag{22}$$

in this paper, the penetration level of the IEEE test feeders is set at 10%.

The first controlled transient was a 0.1 p.u. step in frequency at the point of connection of the distribution system at 0.5 s, while voltage was held constant (Figs. 6 and 7). The second controlled transient was a 0.1 p.u. step in voltage at the point of connection of the distribution system at 0.5 s, while frequency was relatively stable during each transient (Figs. 9, 11 and 12).

The IEEE 34 node test feeder is an actual feeder. The feeder's nominal voltage is 24.9 kV. It is characterized by very long and lightly loaded.

The IEEE 123 node test feeder operates at a nominal voltage of 4.16 kV. It does provide voltage drop problems that must be solved with the application of voltage regulators and shunt capacitors.

Fig. 12 shows the response to a 10% step of system voltage.

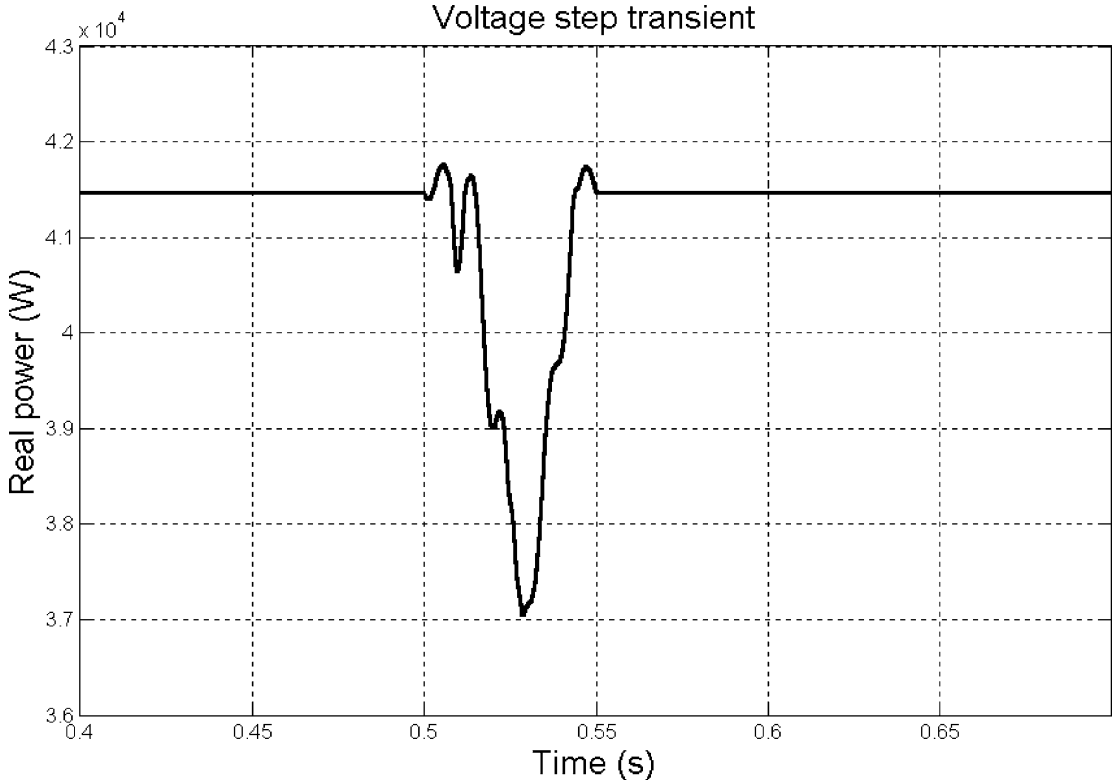

Fig. 9. Fuel cell response to a voltage step transient at node 848 for the IEEE 34 node feeder.

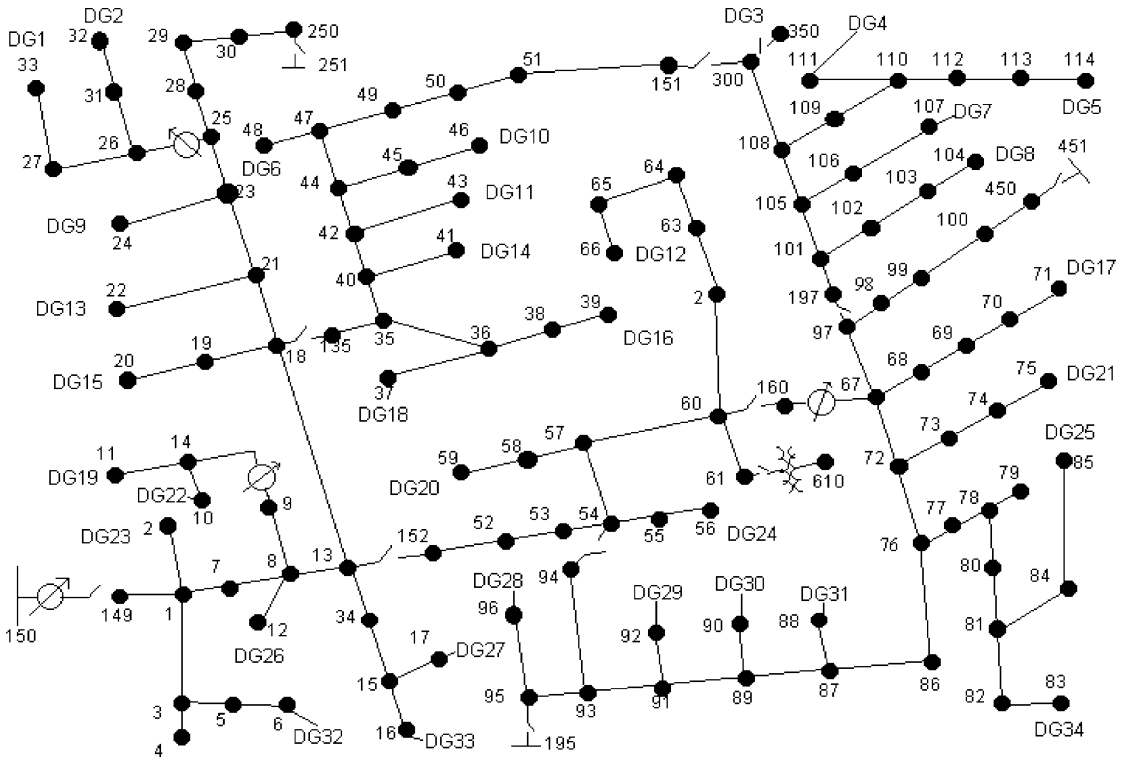

Fig. 10. One line diagram of IEEE 123 node feeder with fuel cells.

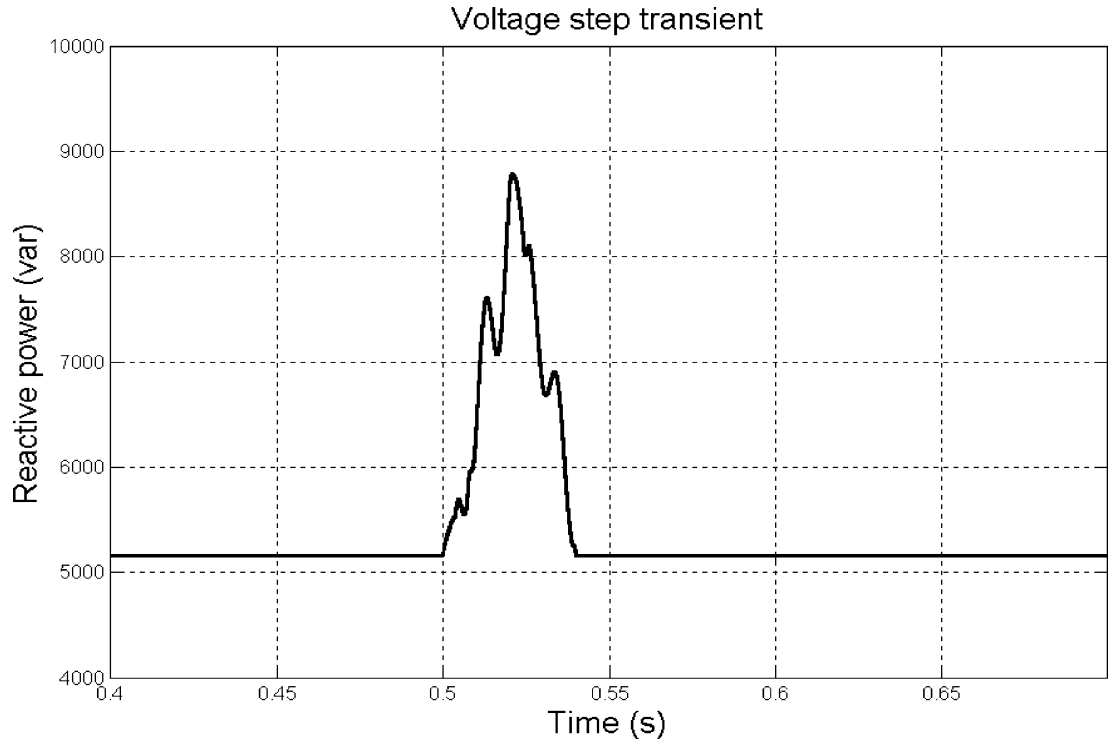

Fig. 11. Fuel cell response to a response for a voltage step transient at node 46 for the IEEE 123 node feeder.

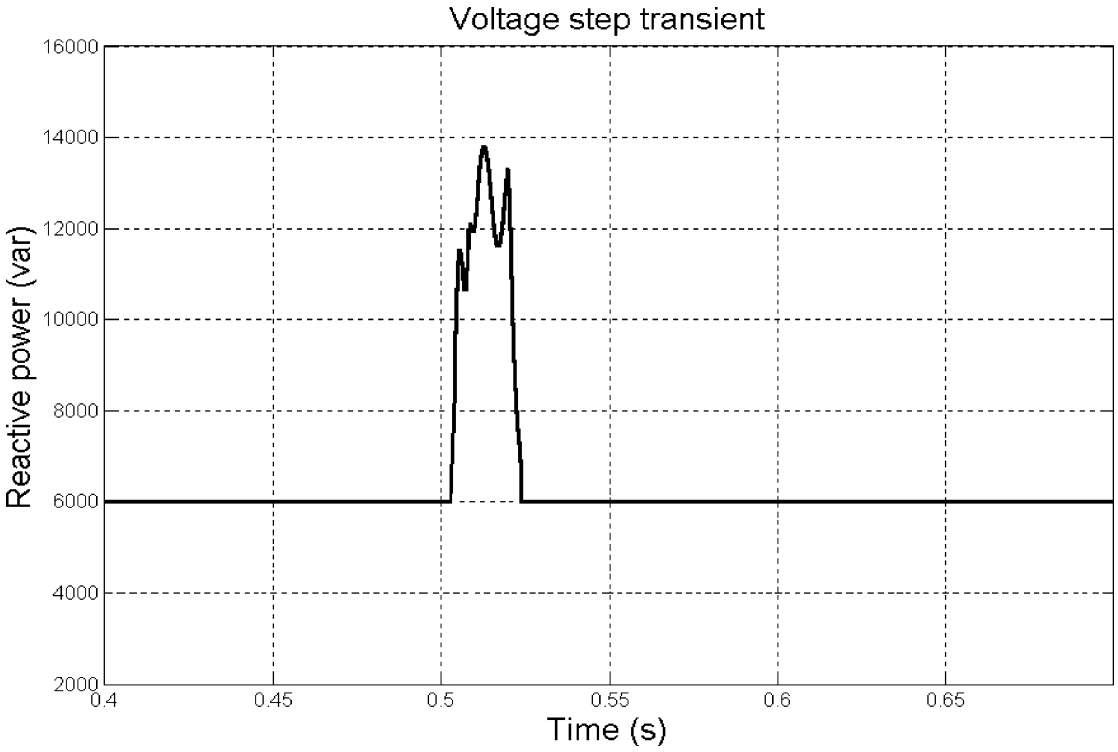

Fig. 12. Fuel cell response to a voltage step transient at node 634 for the IEEE 13 node feeder.

7. Conclusions

The capability to calculate low-order equivalent linear systems from time domain simulations of SOFC models using the ARX algorithm has been established. After the SOFC model was created, it was reduced to transfer functions using the ARX algorithm; thus, the transfer function (reduced-order model) exhibited the same dynamic response as the original SOFC model.

A significant reduction in the model order was achieved. The time domain response of the identified system matches the response of the actual system.

Therefore, each SOFC reduced-order model influences the grid in the same manner as SOFC and loads would, modulating real and reactive power in response to voltage and frequency changes on the grid.

References

[1] F. Jurado, Power supply quality improvement with a SOFC plant by neural-network-based control, J. Power Sour. 117 (1-2) (2003) 75–83.

[2] J.R. Smith, J.F. Hauer, D.J. Trudnowski, Transfer function identification in power system applications, IEEE Trans. Power Syst. 8 (3) (1993) 1282–1290.

[3] M. Bounou, S. Lefebvre, R.P. Malhame, A spectral algorithm for extracting power system modes from time recordings, IEEE Trans. Power Syst. 7 (2) (1992) 665–672.

[4] J.J. Sanchez-Gasca, J.H. Chow, Computation of power system low- or micro-turbine models from time domain simulation using a Hankel matrix, IEEE Trans. Power Syst. 12 (4) (1997) 1461–1467.

[5] D.J. Trudnowski, M.K. Donnelly, J.F. Hauer, A procedure for oscillatory parameter identification, IEEE Trans. Power Syst. 9 (4) (1994) 2049–2055.

[6] J.J. Sanchez-Gasca, J.H. Chow, Performance comparison of three identification methods for the analysis of electromechanical oscillations, IEEE Trans. Power Syst. 14 (3) (1999) 995–1002.

[7] L. Ljung, T. Glad, Modeling of Dynamic Systems, Prentice-Hall, Englewood Cliffs, NJ, 1994.

[8] L. Ljung, System Identification—Theory for the User, 2nd ed., Prentice-Hall, Upper Saddle River, NJ, 1999.

[9] T. Söderström, P. Stoica, System Identification, Prentice-Hall International, London, 1989.

[10] MATLAB, High-performance numeric computation and visualization software, The Mathworks Inc., Natick, MA, 2001.

[11] A.F. Massardo, F. Lubelli, Internal reforming solid oxide fuel cell–gas turbine combined cycles (IRSOFC–GT). Part A. Cell model and cycle thermodynamic analysis, J. Eng. Gas Turbines Power 122 (27) (2000) 27–35.

[12] J. Padullés, G.W. Ault, J.R. McDonald, An integrated SOFC plant dynamic model for power systems simulation, J. Power Sour. 86 (1–2) (2000) 495–500.

[13] S. Campanari, Thermodynamic model and parametric analysis of a tubular SOFC module, J. Power Sour. 92 (1–2) (2001) 26–34.

[14] A.D. Rao, G.S. Samuelsen, Analysis strategies for tubular solid oxide fuel cell based hybrid systems, J. Eng. Gas Turbines Power 124 (3) (2002) 503–509.

[15] Y. Zhu, K. Tomsovic, Development of models for analyzing the load-following performance of microturbines and fuel cells, Elect. Power Syst. Res. 62 (1) (2002) 1–11.

[16] M.C. Chandorkar, New techniques for inverter flux control, IEEE Trans. Ind. Appl. 37 (3) (2001) 880–887.

[17] T. Knudsen, A new method for estimating ARMAX models, in: Proceedings of the 1994 IFAC Symposium on System Identification, Copenhagen, Denmark, pp. 611–617.

[18] P. Stoica, T. Soderstrom, B. Friedlander, Optimal instrumental variable estimates of the AR-parameters of an ARMA process, IEEE Trans. Automat. Contr. 30 (11) (1985) 1066–1074.
[19] P. Van Overschee, B. DeMoor, Subspace Identification of Linear Systems: Theory, Implementation, Applications, Kluwer Academic Publishers, Dordrecht, 1996.
[20] W.H. Kersting, Radial distribution test feeders, in: Proceedings of the 2001 IEEE/PES Summer Meeting, vol. 2, pp. 908–912.
[21] J.A. Kuipers, in: Proceedings of the 1998 Fuel Cell Seminar, 1998, p. 450.
[22] S.C. Singhal, Progress in tubular solid oxide fuel cell technology, in: Proceedings of the 1999 Solid Oxide Fuel Cells, Honolulu, HI, USA, October 17–22, 1999, pp. 39–51.
[23] M.K. Donnelly, J.E. Dagle, D.J. Trudnowski, G.J. Rogers, Impacts of the distributed utility on transmission system stability, IEEE Trans. Power Syst. 11 (2) (1996) 741–746.